



Universiteit
Leiden
The Netherlands

Seizures, spreading depolarizations and sudden death

Jansen, N.A.

Citation

Jansen, N. A. (2026, March 11). *Seizures, spreading depolarizations and sudden death*. Retrieved from <https://hdl.handle.net/1887/4297304>

Version: Publisher's Version

License: [Licence agreement concerning inclusion of doctoral thesis in the Institutional Repository of the University of Leiden](#)

Downloaded from: <https://hdl.handle.net/1887/4297304>

Note: To cite this publication please use the final published version (if applicable).



A stylized, grayscale graphic of a brain, showing the cerebral cortex and internal structures, positioned on the left side of the page.

Chapter 5

Apnea associated with
brainstem seizures in
Cacna1a^{S218L} mice is caused
by medullary spreading
depolarization

Nico A. Jansen

Maarten Schenke

Rob A. Voskuyl

Roland D. Thijs

Arn M.J.M. van den Maagdenberg

Else A. Tolner

J Neurosci 2019;39(48):9633-9644

ABSTRACT

Seizure-related apnea is common and can be lethal. Its mechanisms however remain unclear and preventive strategies are lacking. We postulate that brainstem spreading depolarization (SD), previously associated with lethal seizures in animal models, initiates apnea upon invasion of brainstem respiratory centers. To study this, we assessed effects of brainstem seizures on brainstem function and respiration in male and female mice carrying a homozygous S218L missense mutation that leads to gain-of-function of voltage-gated $\text{Ca}_v2.1 \text{ Ca}^{2+}$ channels and high risk for fatal seizures. Recordings of brainstem DC potential and neuronal activity, cardiorespiratory activity and local tissue oxygen were performed in freely behaving animals. Brainstem SD occurred during all spontaneous fatal seizures and, unexpectedly, during a subset of non-fatal seizures. Seizure-related SDs in the ventrolateral medulla correlated with respiratory suppression. Seizures induced by stimulation of the inferior colliculus could evoke SD that spread in a rostral-caudal direction, preceding local tissue hypoxia and apnea, indicating that invasion of SD into medullary respiratory centers initiated apnea and hypoxia rather than *vice versa*. Fatal outcome was prevented by timely resuscitation. Moreover, NMDA receptor antagonists MK-801 and memantine prevented seizure-related SD and apnea, which supports brainstem SD as a prerequisite for brainstem seizure-related apnea in this animal model and has translational value for developing strategies that prevent fatal ictal apnea.

INTRODUCTION

Seizure-related apnea occurs commonly in patients with epilepsy and can result in severe hypoxemia.¹⁻³ If prolonged, apnea may be fatal, as such apnea preceded cardiac arrest in rarely monitored cases of ‘sudden unexpected death in epilepsy’ (SUDEP),⁴ a fatal complication of epilepsy affecting patients of all ages.⁵⁻⁷ Seizure-related apnea, however, has a benign outcome in the large majority of cases, yet given its presumed role in SUDEP there is an urgent need to understand mechanisms of potentially lethal respiratory suppression. Neuropathological and structural neuroimaging changes⁸⁻¹⁰ in brainstem regions of SUDEP cases suggest seizure-related brainstem dysfunction as a possible critical factor leading to fatal apnea.

In recent years, brainstem spreading depolarization (SD) has been linked to SUDEP based on studies in various transgenic mouse models. A negative DC-potential shift in the dorsal brainstem was observed indicating brainstem SD.^{11, 12} In these studies, SD appeared to follow upon severe respiratory compromise, thereby providing an explanation for the absence of autoresuscitation following apnea.¹¹ Brainstem SD was also demonstrated for cortically induced and spontaneous fatal seizures in mice harboring the homozygous S218L gain-of-function missense mutation in the *Cacna1a* gene that encodes the α_{1A} subunit of voltage-gated $\text{Ca}_v2.1$ Ca^{2+} channels.¹³ The absence of cortical seizure activity in this model suggests an important role for brainstem circuitry in the genesis of seizures. However, it remains an enigma whether changes in breathing rhythm result in hypoxia and trigger brainstem SD, or *vice versa*, which is key when considering strategies for (preventative) interventions of seizure-related apnea.

Breathing rhythm is generated by the ventral respiratory column, located in the ventrolateral medulla (VLM).^{14, 15} The preBötzinger complex (preBötC), a sub-region of the VLM, specifically generates the inspiratory phase that is crucial for respiratory function.¹⁵⁻¹⁸ Rapid suppression of glutamatergic preBötC neurons induces fatal apnea.¹⁹ We postulate that seizure-induced brainstem SD can evoke apnea due to prolonged neuronal suppression in the VLM. To test this, we studied brainstem neuronal activity and cardiorespiratory function during spontaneous seizures and seizures induced by stimulation of the inferior colliculus in freely behaving homozygous *Cacna1a*^{S218L} mice. Reversibility of brainstem SD was evaluated by mechanical ventilation during apnea. Since brainstem SD commonly preceded apnea and local hypoxia, we also tested whether increasing the SD threshold by NMDA antagonism could prevent lethality.

MATERIALS AND METHODS

Animals

Missense mutation S218L was introduced in the mouse *Cacna1a* gene, generating *Cacna1a*^{S218L} mice, using a gene-targeting approach.²⁰ Mice were backcrossed to C57BL/6J for at least 10 generations and both male and female mice, age 3 to 6 months, were used in experiments. Standard housing conditions and a 12-h light/dark cycle with food and water available *ad libitum* were applied. Experiments were approved by local and national ethical committees in accordance with recommendations of the European Communities Council Directive (2010/63/EU) and carried out in accordance with ARRIVE guidelines.

Surgery for recordings of spontaneous seizures

Cacna1a^{S218L} mice (15 males and 17 females) were implanted with either 7 ($n = 11$) or 16 ($n = 21$) electrodes (single or paired 75 μm platinum/iridium, PT6718; Advent Research Materials) under isoflurane anesthesia (induction 4%; maintenance 1.5%). Electrode configurations were as follows (coordinates relative to bregma; in mm anterior, lateral and ventral, respectively): for 7-channel recordings (E363/0 socket contacts and MS373 pedestal; Plastics One), electrodes were implanted in right primary visual cortex (V1; -3.5/2.0/0.5; unipolar) and oral pontine reticular nucleus (PnO; -4.8/0.8/3.7; uni- or bipolar) and VLM (-6.7/1.3/4.1; uni- or bipolar); for 16-channel recordings (#0489 pin receptacles and #831 18-pin pedestal; Mill-Max), unipolar electrodes were implanted in right V1 and bilaterally in primary motor cortex (+1.5/1.8/0.6), hippocampus (-2.2/2.0/1.3) and amygdala (-1.7/2.9/4.0), with bipolar electrodes in right inferior colliculus (IC; -5.0/1.0/0.6), PnO and VLM. Electrodes inserted bilaterally above the cerebellum served as reference and ground. For ECG, electrodes were placed in the flank. For respiratory recordings ($n = 13$), a thermistor probe (MEAS-G22K7MCD419, Measurement Specialties) was inserted above the epithelium of the anterior nasal cavity as described previously.²¹ The pedestal was secured to the skull using dental cement (DiaDent Europe). In a subset of animals ($n = 14$), cerebral blood flow (CBF) was measured using an optic fiber (200 μm , CFM12L02; Thorlabs, Newton, NJ) placed on the dura overlaying V1. Postoperative analgesia was supplied with carprofen and buprenorphine (5 mg/kg and 0.1 mg/kg respectively, s.c.). Electrode configurations were first tested in wildtype mice for a 2-week period.

Surgery for recordings of induced seizures

For IC stimulation in homozygous *Cacna1a*^{S218L} and wildtype animals, bipolar electrodes were randomly implanted in the left or right IC. Two electrode configurations were used, with i) bipolar electrodes bilaterally in VLM, or ii) electrodes implanted unilaterally in VLM (bipolar) and the rostral and caudal parvicellular reticular nucleus (unipolar; PCRT-r, -5.5/1.4/3.6; PCRT-c, -6.1/1.3/4.0) to create an array of brainstem electrodes ipsilateral to the stimulated IC. An unipolar electrode in right V1 and a nasal thermistor were implanted as described above. Two to 4 days after surgery, a 50-Hz train of 1-ms bipolar pulses was delivered through the IC electrode for 2

s. Threshold for seizure-related behavior, which consistently commenced with wild running, was determined for a range of intensities of [30 50 100 200 500] μA with 10 min between subsequent pulse trains. The threshold current was delivered twice daily for 3 days, but limited to one stimulation in case of a generalized tonic-clonic seizure. In a separate group of *Cacna1a*^{S218L} mice, local oxygen partial pressure (pO_2) was measured using a technique involving oxygen quenching of fluorescence generated in a platinum-based dye in the tip of an optic fiber (Oxylite; Oxford Optronics). This allows for absolute measurements of pO_2 without consuming oxygen.²² Probes (230 μm), pre-calibrated by the manufacturer and indicated with a T90 response time (i.e. time to reach 90% of the actual pO_2 change) of less than 20 s, were inserted rostral of the VLM electrode (-6.2/1.3/3.8), replacing the PCRt-c electrode. To study the locality of changes in pO_2 , a subset of mice was implanted with a second oxygen probe in V1, anterior to the V1 electrode (-3.0/2.0/0.5).

Surgery for recordings of cortically induced SD

For cortical SD induction, a subset of homozygous *Cacna1a*^{S218L} mice was implanted with a bipolar electrode in V1 and unipolar electrodes in the primary somatosensory cortex (S1; -0.5/2.0/0.5) and M1. Directly adjacent to the S1 electrode, an oxygen probe was implanted. Cathodal stimulation (100 μA for 1 s) was administered once daily for 1 or 2 days and reliably resulted in cortical SD.

Mechanical ventilation and pharmacology

Postictal respiratory support (150 breaths/min for 20 – 50 s, 250 μL per breath) was administered via the nostrils by a polyethylene tube connected to a mechanical ventilator (Mini-Vent; Harvard Apparatus). In a sham group, the same procedure was performed with the ventilator switched off.

To test the effects of NMDA receptor antagonists on seizure behavior and outcome, mice that showed brainstem SD in response to initial IC stimulation were used. Vehicle, MK-801 (1 mg/kg BW) or memantine hydrochloride (10 mg/kg BW; both from Sigma-Aldrich) were injected i.p. 30 min prior to IC stimulation by an experimenter blinded to the treatment.

Histology

Surviving animals were euthanized by CO_2 . Electrolytic lesions were made at the tip of brain electrodes (10- μA anodal current) in all animals to enable confirmation of electrode positions. After transcardial perfusion (for euthanized animals), brains were post-fixed in 4% paraformaldehyde for 2.5 h at room temperature, or for 24 h at 4°C (for spontaneously deceased animals), and sucrose-processed. Coronal brain sections (40 μm) were made using a sliding microtome (Leica) and Nissl-stained to confirm electrode positions.

Data acquisition and analyses

Immediately following surgery, animals were connected to a commutator (ACO32 for 16-channel recordings; Tucker-Davis Technologies; a custom-made system was used for 7-channel recordings). Data were amplified and digitized as described previously.²³ Recordings of pO_2 were acquired at 1 Hz.

SD was defined as a transient negative DC-shift with amplitude >5 mV measured with a delay at 2 recording locations, or limited to one location if accompanied by depression of local multi-unit activity (MUA). Video-EEG recordings during these events and the 24 h preceding the fatal seizure were analyzed for seizures, which were scored using the Racine-scale.²⁴ In retrospect, all fatal seizures were of stage 5 and hence stage 5 non-fatal seizures were used for comparative analyses. Single seizures or seizure clusters lasting more than 30 min were regarded as status epilepticus²⁵ and, as a SUDEP exclusion criterion,²⁶ excluded from further analyses.

Electrophysiological data were analyzed using custom-written MATLAB (MathWorks) scripts. For ECoG power analyses, AC-signals were artifact-rejected, digitally low-pass filtered (Chebyshev IIR 8th order filter) and down-sampled to 500 Hz. Total ECoG power (1-100 Hz) was calculated using a Fast Fourier Transform. For MUA, the root mean square was computed over 10 or 100 ms. Peak detection was used to determine instantaneous heart rate and respiratory rate from ECG and thermistor recordings respectively. For heart rate variability (HRV) analyses, standard deviation of all normal ECG R-R intervals (SDNN) was calculated.²⁷ Pre- and postictal parameters were calculated over 5-min periods. Longer-term heart rhythm changes were not analyzed, as HRV is profoundly increased during the first week following surgery.²⁷ Peri-ictal CBF, MUA and ECoG power were normalized by activity levels during a 1-min period 5 min pre-ictal. For ECoG and CBF analyses, seizures associated with cortical SD were excluded due to local SD-related suppression.

Experimental design and statistical analysis

In total, data from 104 mice were included: recordings from spontaneous seizures were obtained from 32 homozygous *Cacna1a*^{S218L} mice, while seizures were induced in 68 mice (3 wildtype and 65 homozygous *Cacna1a*^{S218L} mice), including 12 mice for mechanical ventilation and 31 mice for pharmacological experiments. A maximum of 3 seizures were induced in untreated animals, while 1 seizure was induced for experiments involving respiratory or pharmacological intervention. Cortical SD induction was performed in 4 homozygous *Cacna1a*^{S218L} mice.

Statistical testing was performed using MATLAB or GraphPad Prism (GraphPad Software). Data are represented as mean \pm SEM in text and time series graphs, total range for box-and-whisker graphs and mean \pm S.D. for graphs showing individual data points. Data are compared using 2-tailed paired or unpaired Student's *t*-tests, or one-way ANOVA with Dunnett's post-hoc test for multiple comparisons, unless indicated otherwise. $p < 0.05$ was considered significant.

RESULTS

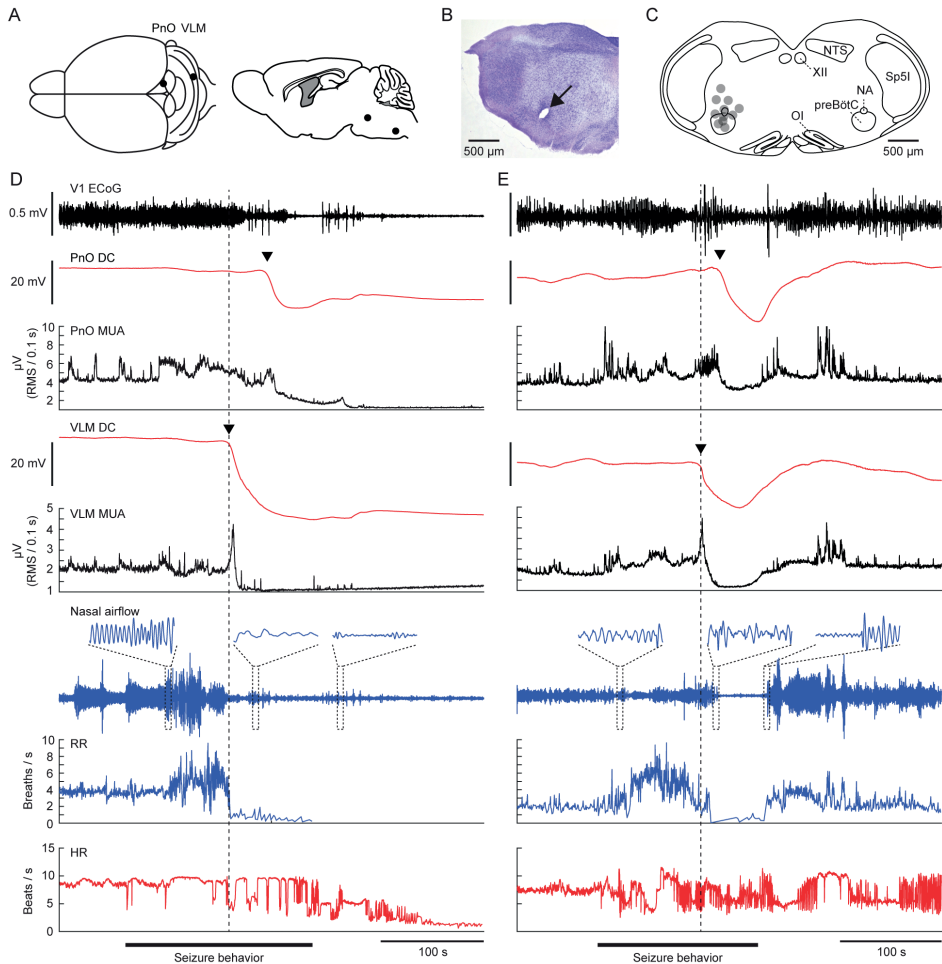
Brainstem SD occurs during seizures in freely behaving *Cacna1a*^{S218L} mice

Over a 2-week recording period, 63% (20/32) of implanted *Cacna1a*^{S218L} mice died after a mean survival period of 2.7 ± 0.5 days (range: 8 h – 9 days). High mortality in the days following surgery in this model was earlier described to be seizure-related.¹³ Indeed, mice died following a Racine stage 5 seizure ($n = 15$; 8 males and 7 females) or status epilepticus ($n = 5$; 2 males and 3 females). All fatal seizures were accompanied by SDs in brainstem areas including the PnO (11/11 recordings) and VLM (13/13 recordings; Fig. 1A-D) and occasionally IC (3/7 recordings). In contrast, SDs were observed in forebrain areas (neocortex, hippocampus and amygdala) in only 7/15 fatal seizures and during status epilepticus (5/5). All brainstem SDs occurred during seizure behavior, with behavioral arrest starting 84 ± 17 s (range: 15 – 160) after onset of VLM SD and 67 ± 18 s (range: 4 – 142) after PnO SD.

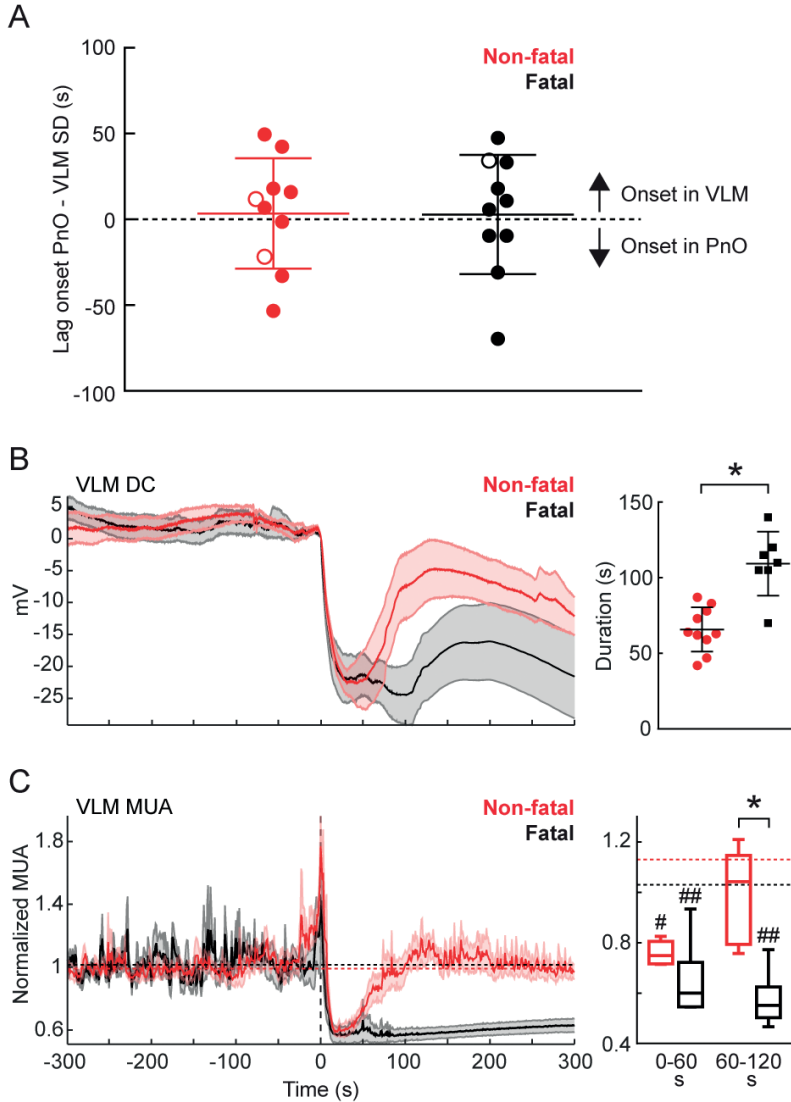
To assess whether brainstem SD was unique for fatal events, we inspected recordings of the 24 h preceding the fatal events. Out of 64 non-fatal stage 5 seizures ($n = 12/15$ animals [range: 1 – 12 per animal]), 19% were accompanied by brainstem SD ($n = 12$ in 7 animals; Fig. 1E). The duration of seizures accompanied by brainstem SD was similar to that of seizures without brainstem SD and fatal seizures (185 ± 24 , 170 ± 23 and 194 ± 25 s, respectively; $p = 0.525$; ANOVA). Brainstem SD was never observed during seizures of lower Racine stage or during interictal periods.

Prolonged SD in the ventrolateral medulla is associated with lethal outcome

In all fatal and in most (10/12) non-fatal seizures, parallel DC recordings in the PnO and VLM demonstrated SD in both brainstem areas. During 2 non-fatal seizures, only PnO SD occurred, suggesting that during non-fatal seizures SD in the brainstem remains more local than for fatal seizures. Delay between SD onset in PnO and VLM did not indicate evidence for a consistent spreading pattern during non-fatal or fatal seizures: delay was variable and SD could be first detected in either of the 2 areas (Fig. 2A), indicating that the origin of SD may vary for spontaneous seizures. Duration of VLM SD, as measured from SD onset to partial (20%) recovery of DC-potential, was longer for fatal compared to non-fatal seizures (Fig. 2B).

FIGURE 1. Brainstem spreading depolarization (SD) and cardiorespiratory dysfunction during a spontaneous fatal and non-fatal seizure in a *Cacna1g*^{S218L} mutant.

(A) Top and sagittal view of experimental approach for chronic brainstem recordings. (B) Nissl staining showing a lesion marking the electrode tip in the ventrolateral medulla (VLM; arrow). (C) Schematic of VLM electrode positions (grey dots) in 11 *Cacna1g*^{S218L} mice that died following a spontaneous fatal seizure with VLM SD (NA = nucleus accumbens; NTS = nucleus tractus solitarius; OI = oliva inferior; preBötC = pre-Bötzinger complex; Sp5l = spinal trigeminal nucleus pars interpolaris; XII = nucleus hypoglossus). (D) Example of a fatal seizure showing brainstem SD, evidenced by a DC shift (arrowheads), in the oral pontine reticular nucleus (PnO) and VLM. Note that the SDs occurred during seizure behavior, and were associated with a transient increase in multi-unit activity (MUA) followed by suppression (ECoG = electrocorticogram; HR = heart rate; RR = respiratory rate; RMS = root mean square; V1 = primary visual cortex). (E) Example of a non-fatal seizure that was associated with brainstem SD, after which DC-potential and MUA spontaneously recovered. Note that in both fatal and non-fatal examples, respiratory activity decreased shortly after onset of VLM SD (indicated by dashed line).

FIGURE 2. Prolonged medullary neuronal depression following fatal spreading depolarization (SD) in *Cacna1a*^{S218L} mice.

(A) Brainstem SD was observed first in either the ventrolateral medulla (VLM) (positive values) or in the oral pontine reticular nucleus (PnO) (negative values) during non-fatal ($n = 10$) and fatal ($n = 10$) seizures. This variability was observed between animals and within animals, as illustrated by the data points from a single animal with a fatal and 2 non-fatal seizures associated with brainstem SD (open symbols). (B) Averaged DC-recordings in VLM showing SD (left; onset at time = 0 s), indicating earlier recovery for non-fatal ($n = 10$) compared to fatal ($n = 10$) seizures (right; 66 ± 15 s versus 109 ± 21 s, $t(15) = 5.03$, $*p = 0.0001$, unpaired t -test). Note that DC-recordings from three fatal seizures were excluded due to absence of (partial) recovery. (C) For fatal versus non-fatal seizures, VLM multi-unit activity (MUA) was reduced after SD onset in both groups (right; $n = 5$ and $n = 6$; baseline indicated by dashed lines; $*p = 0.009$, $**p = 0.0003$ and $**p = 0.0004$ respectively, ANOVA with Dunnett's test), but then recovered only in non-fatal cases ($t(9) = 4.62$, $*p = 0.001$, unpaired t -test).

Seizures with brainstem SD confer decreased survival and are followed by ECoG suppression and increased heart rate variability

The time towards a fatal seizure was decreased following non-fatal seizures accompanied by brainstem SD when compared to other stage 5 seizures (4.6 ± 1.1 and 6.3 ± 1.3 h, respectively; $t(11) = 2.55$, $p = 0.031$, paired t -test). Behaviorally, the majority of non-fatal seizures with brainstem SD terminated with a hindlimb clonus (10/12; all in seizures with VLM SD), a finding previously reported for fatal seizures in *Cacna1a*^{S218L} mice.¹³ Onset of hindlimb clonus and VLM SD were closely aligned (Fig. 3A). Pairwise comparisons of pre- and postictal parameters of stage 5 seizures with and without brainstem SD revealed that V1 ECoG was suppressed during the postictal period specifically for seizures with brainstem SD, whereas no differences in cortical CBF was observed (Fig. 3B). Postictal heart rate variability (HRV) was increased for seizures with brainstem SD, while heart rate remained constant (Table 1). In addition, skipped heart beats occurred more often in the postictal period for seizures with brainstem SD (example in Fig. 3C,D) when compared to seizures without brainstem SD (Table 1).

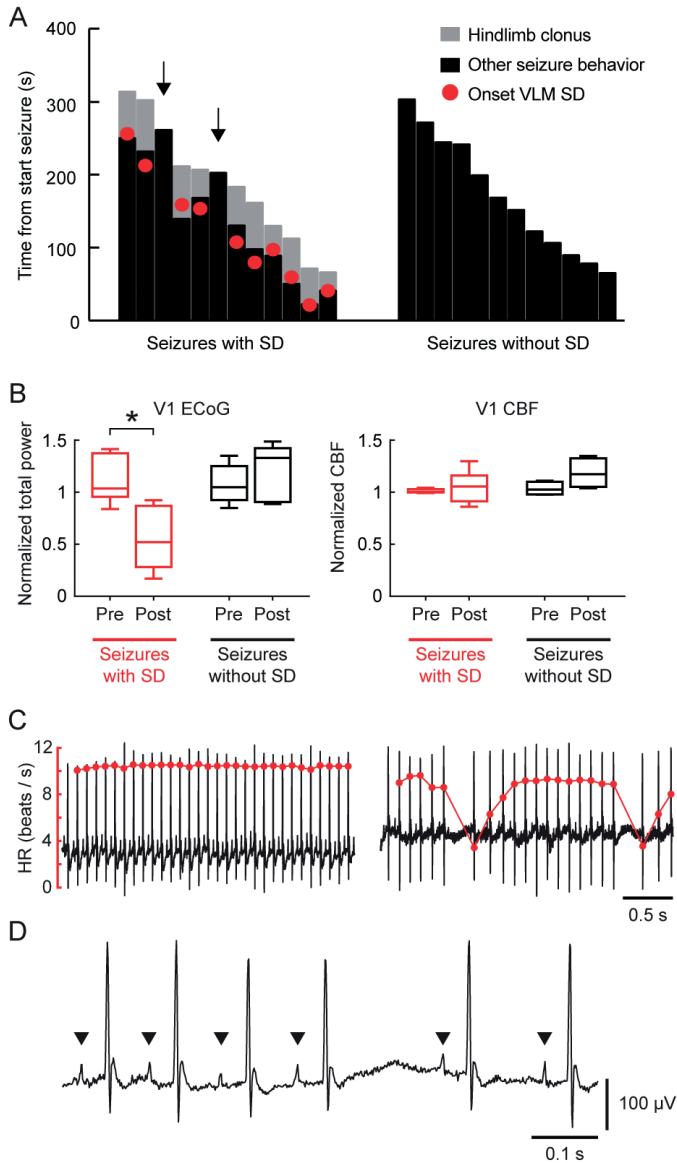
Seizure-related bradypnea correlates with SD in the ventrolateral medulla

Respiratory activity was recorded in a subset of mice with a spontaneous fatal seizure ($n = 6$). In 4 mice, 8 non-fatal seizures with brainstem SD occurred: 2 with SD restricted to the PnO and 6 with SD occurring in both PnO and VLM. All seizures with SD in the VLM were associated with bradypnea (defined as <60 breaths/min), in contrast to the cases with SD limited to PnO (example in Fig. 4). Dynamics of VLM SD more closely paralleled changes in respiratory rate when compared to PnO SD (Fig. 5A,B). In a case with strong coupling of oscillatory VLM MUA and breathing rhythm, VLM SD induced immediate cessation of this oscillatory pattern coinciding with bradypnea onset (Fig. 5C). In contrast to the profound respiratory effects, prolonged bradycardia was not observed for non-fatal seizures with VLM SD, while occurring after about one minute following fatal apnea for fatal seizures (Fig. 5D,E).

TABLE 1. Postictal changes in heart rhythm after brainstem spreading depolarization (SD).

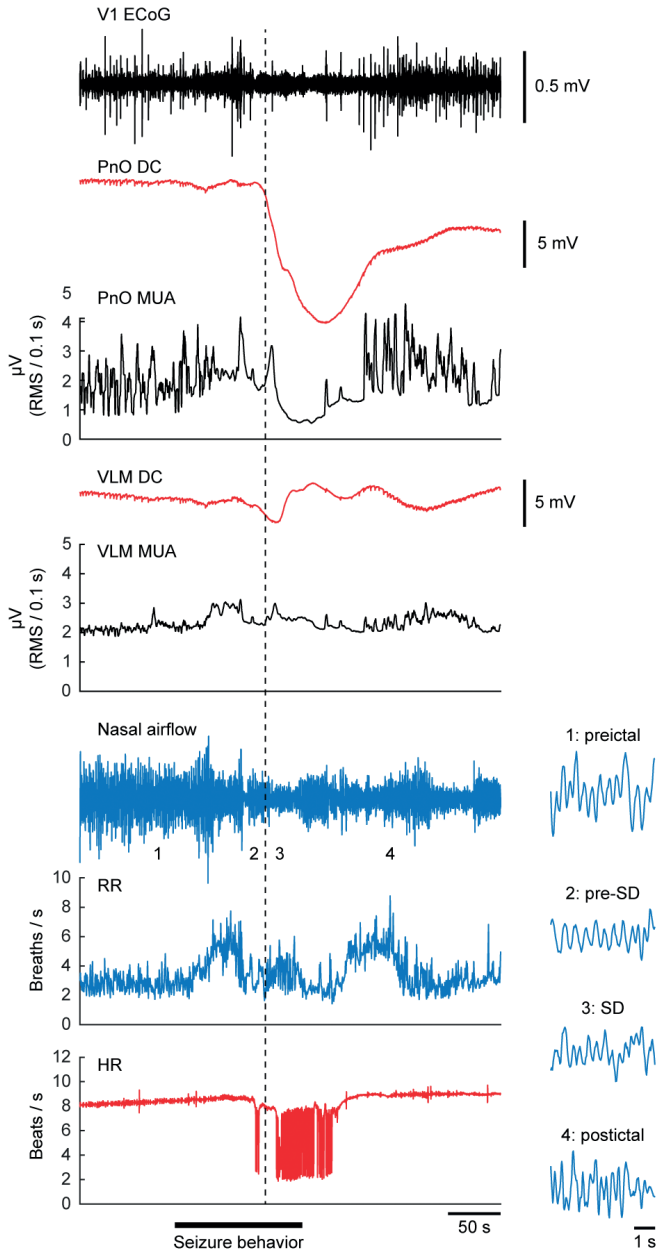
Mice	Seizures	Heart rate (beats/s)		Heart rate variability (SDNN [ms])		Skipped heart beats (total count)	
		Pre-ictal	Postictal	Pre-ictal	Postictal	Pre-ictal	Postictal
Seizures with brainstem SD							
6	9	8.12 ± 0.53	7.39 ± 0.34	22.8 ± 4.8	$45.1 \pm 7.0^*$	6.50 ± 4.13	$65.5 \pm 28.5^{**}$
Seizures without brainstem SD							
6	9	8.37 ± 0.33	8.44 ± 0.49	20.2 ± 4.4	22.0 ± 3.6	6.61 ± 2.72	6.13 ± 2.80

* $p = 0.016$, ** $p = 0.008$ for pre-ictal versus post-ictal via Wilcoxon test.
SDNN = standard deviation of all normal ECG R-R intervals

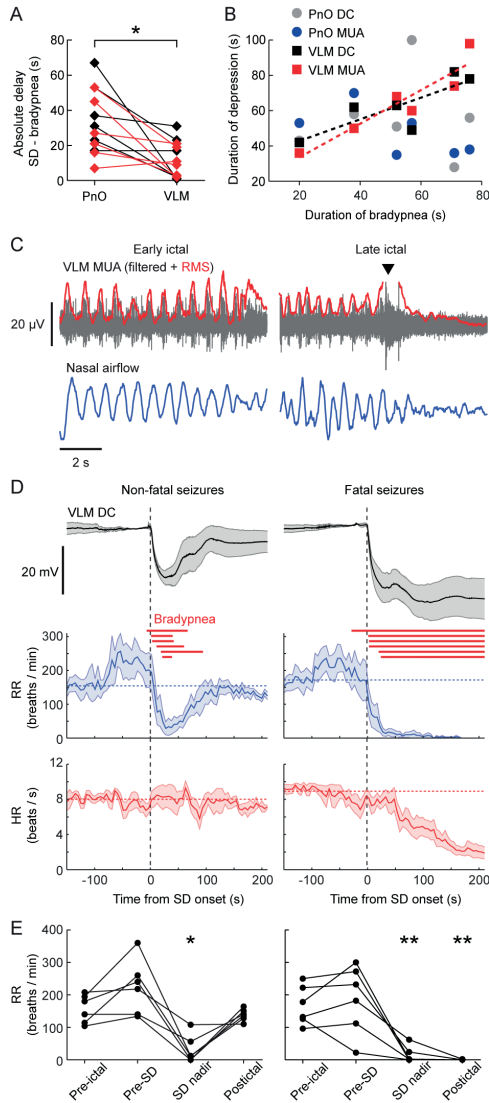
FIGURE 3. Seizure behavior and postictal dynamics indicate brainstem spreading depolarization (SD) during non-fatal seizures in *Cacna1a*^{S218L} mice.

(A) Duration of hindlimb clonus and other seizure behavior for seizures with and without brainstem SD, indicated from onset of seizure behavior (at time = 0 s). Hindlimb clonus only occurred during seizures with SD in ventrolateral medulla (VLM), and started closely to SD onset. Note that hindlimb clonus did not occur during seizures without brainstem SD and seizures with SD restricted to the oral pontine reticular nucleus (PnO; $n = 2$; arrows). **(B)** Electroencephalogram (ECoG) power was significantly suppressed during the postictal period for seizures with brainstem SD ($t(7) = 5.74$, $*p = 0.001$, paired t -test), whereas no difference was present for seizures without brainstem SD. Cortical blood flow (CBF) was not significantly different (V1 = primary visual cortex). **(C)** Examples of ECG signal (black) and heart rate (HR; red) during a pre-ictal (left) and postictal (right) period of a non-fatal seizure with brainstem SD, showing bradyarrhythmias. **(D)** Example of postictal ECG signal showing P-waves (indicated by arrowheads) and their absence during a prolonged R-R pause.

FIGURE 4. Isolated spreading depolarization (SD) in the rostral brainstem during a spontaneous non-fatal seizure.

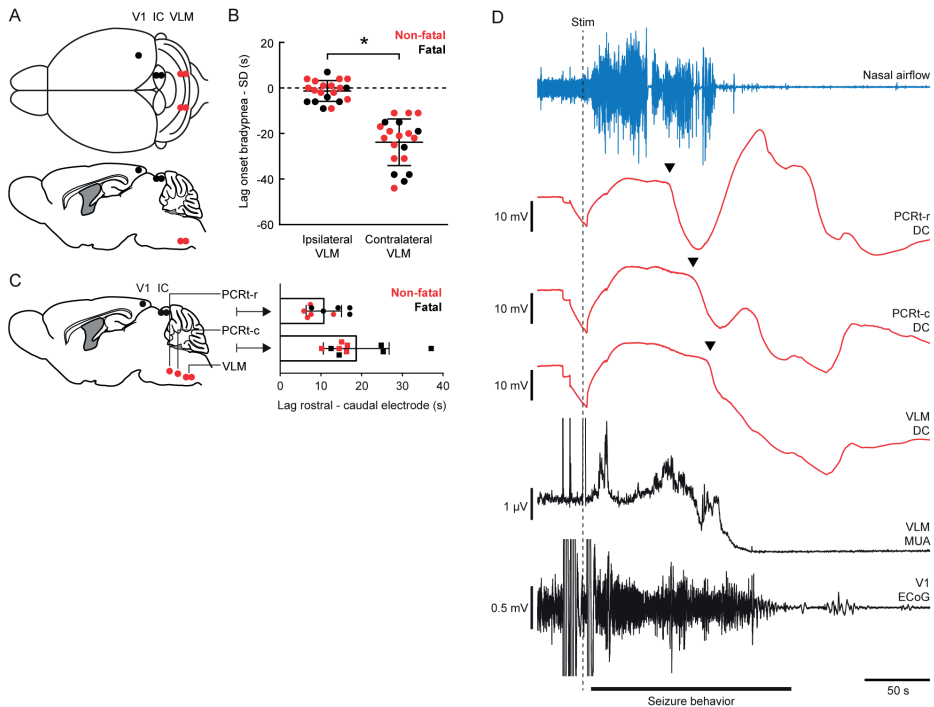


Example of a non-fatal seizure with SD (dashed line) in the oral pontine reticular nucleus (PnO) without evidence of ipsilateral SD in the ventrolateral medulla (VLM). Note that no bradypnea occurred, whereas bradyarrhythmias were observed during and following PnO SD. Insets show details of nasal airflow at time points 1 – 4, indicating no disruption of breathing.

FIGURE 5. Spreading depolarization (SD) in the ventrolateral medulla (VLM) is strongly correlated with seizure-related respiratory suppression in *Cacna1a*^{S218L} mice.

(A) Absolute time delay between onset of bradypnea and SD in the oral pontine reticular nucleus (PnO) and VLM for non-fatal (in red; $n = 6$) and fatal (in black; $n = 6$) seizures, showing that VLM SD occurred significantly closer to onset of bradypnea ($t(11) = 3.64$, $*p = 0.004$, paired t -test). (B) Duration of brainstem DC and multi-unit activity (MUA) depression plotted against duration of bradypnea. Significant correlation was observed only for VLM DC and MUA (dashed lines; $R^2 = 0.671$, $p = 0.046$ and $R^2 = 0.873$, $p = 0.006$, respectively, linear regression). (C) Disruption of phase-coupled MUA in the ventrolateral medulla and breathing during a fatal seizure. In this example, VLM MUA was phase-coupled with nasal airflow. Local MUA (RMS = root mean square) peaked during onset of VLM SD (arrowhead), followed by suppression which coincided with cessation of breathing activity. (D) VLM DC-potential, RR and HR synchronized at onset of non-fatal (left) and fatal (right) VLM SD (at time = 0 s). Red lines indicate bradypnea duration for a fatal seizure. Horizontal dashed lines indicate respiratory rate (RR) and heart rate (HR) during a 60-second pre-ictal period. (E) RR was significantly suppressed during SD nadir, but only for fatal seizures suppression continued into the postictal period (30 s after behavioral arrest; $*p = 0.002$, $**p < 0.001$, ANOVA with Dunnett's test).

FIGURE 6. Stimulation of the inferior colliculus (IC) induces early ipsilateral brainstem spreading depolarization (SD) that propagates from rostral to caudal in *Cacna1a*^{S218L} mice.



(A) Top and sagittal view of experimental approach for IC stimulation in freely behaving mice (V1 = primary visual cortex; VLM = ventrolateral medulla). (B) Time lag in onset of bradypnea (dotted line) and SD in VLM for non-fatal (red) and fatal (black) seizures. Negative values indicate bradypnea preceding SD. Ipsilateral VLM SD always preceded contralateral SD ($t(19) = 9.08$, $*p < 0.0001$, paired t -test), irrespective of laterality ($n = 11$ for left IC, $n = 9$ for right IC). (C) Brainstem array recordings showed SD propagation from the parvocellular reticular nucleus (PCRT) to VLM for all seizures induced by IC stimulation. Time lag between SDs was shorter for the rostral (PCRT-r versus PCRT-c) when compared to the caudal (PCRT-c versus VLM) electrodes ($t(9) = 2.75$, $p = 0.023$, paired t -test). (D) Example recording of a fatal seizure following IC stimulation (dashed line) indicating sequential SDs (arrowheads) in the rostral (top) to caudal (bottom) brainstem electrodes (ECoG = electrocorticogram; MUA = multi-unit activity).

Inferior colliculus stimulation induces brainstem seizures and SD invasion of the ventrolateral medulla coinciding with bradypnea onset

Seizure behavior and absence of cortical epileptiform activity in *Cacna1a*^{S218L} mice suggest an important role for brainstem networks.¹³ We therefore tested whether stimulation of the IC, a component of the brainstem seizure network,^{28, 29} could evoke similar seizure behavior but in a more predictable manner than seen with spontaneous brainstem seizures. Unilateral electrical IC stimulation (Fig. 6A) induced a short-lasting running fit (1 – 3 s) in wildtype mice ($n = 3$), whereas all *Cacna1a*^{S218L} mice ($n = 12$) showed a stage 5 seizure already during threshold testing. Thresholds for running fits and/or behavioral seizure activity were lower in *Cacna1a*^{S218L} than wildtype mice

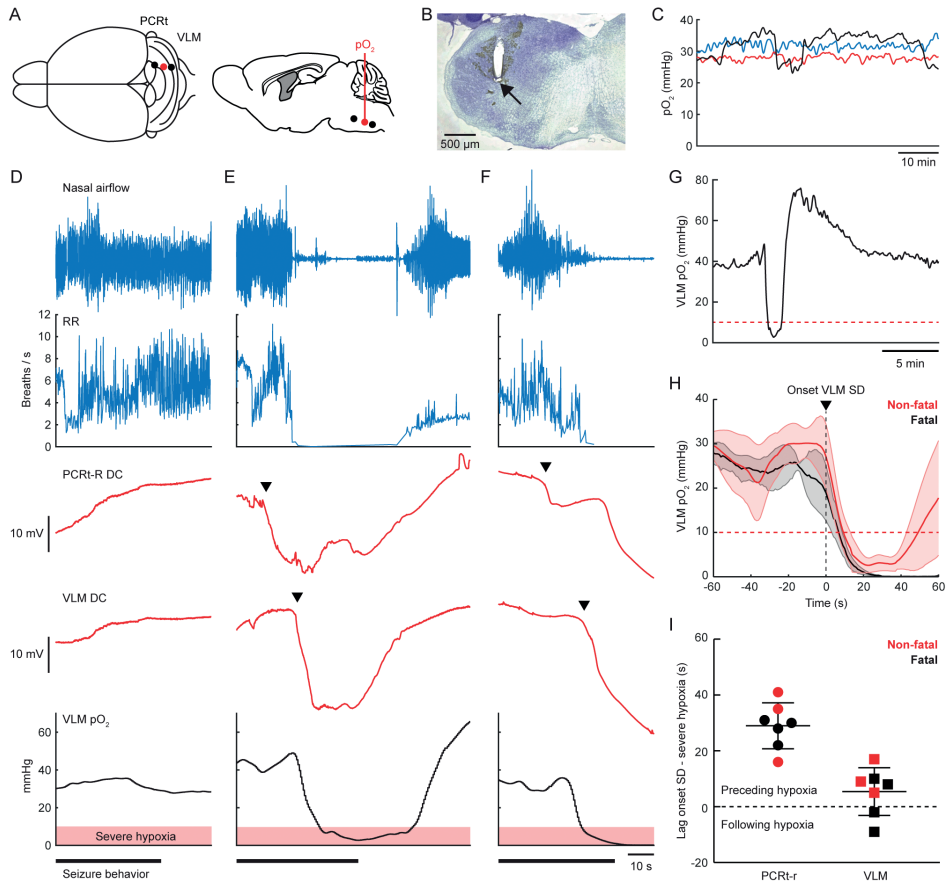
(52 μ A [range 30 – 100 μ A] versus 267 μ A [range 100 – 500] respectively; $p = 0.005$, Mann-Whitney test). In total, 27 seizures were induced in *Cacna1a*^{S218L} mice, of which 20 were non-fatal and 7 fatal. Stimulation resulted in stage 5 seizures that were of comparable duration as spontaneous seizures (133 \pm 11, 162 \pm 6 and 135 \pm 3 s for non-fatal seizures without and with brainstem SD and fatal seizures, respectively), and never associated with cortical SD or epileptiform events.

Bilateral VLM recordings in *Cacna1a*^{S218L} mice revealed SD during all 7 fatal and 13/ 20 non-fatal seizures, with a delay of 106 \pm 3 and 104 \pm 7 s after stimulation, respectively ($t(19) = 0.33$, $p = 0.763$, unpaired t -test). SD never occurred in wildtype mice. Notably, we observed VLM SD first at the site ipsilateral to stimulation, coinciding with bradypnea onset (Fig. 6B), although breathing slowed down already seconds preceding VLM SD. The consistent SD delay between left and right VLM following stimulation contrasts the inconsistent delay between PnO and VLM SD during spontaneous seizures, possibly reflecting lack of a local seizure focus for spontaneous events. Hence, we examined the possibility of spread in a separate group of *Cacna1a*^{S218L} mice with electrodes in the VLM and the rostral and caudal parvocellular reticular nucleus (PCRT-r and PCRT-c, respectively) (Fig. 6C). In all animals stimulated ($n = 8$; 10 seizures with brainstem SD, of which 5 were fatal), we observed SD first in PCRT-r, followed by PCRT-c and VLM (Fig. 6C,D). This indicates that SD spread following IC stimulation is predictable, but variable during spontaneous seizures, in *Cacna1a*^{S218L} mice.

Medullary SD is followed by local hypoxia

Ongoing breathing activity does not rule out impaired oxygenation, which can induce brainstem SD.³⁰ We therefore determined *in situ* brainstem pO_2 immediately rostral to the VLM electrode ($n = 6$ animals; Fig. 7A,B). Following IC stimulation, 7/12 seizures were associated with SD in PCRT-r and VLM, of which 4 were fatal. Baseline pO_2 in the rostral VLM was 34.2 \pm 3.1 mmHg and remained within the normoxic range of 20 – 40 mmHg during non-fatal seizures without brainstem SD (Fig. 7D). During seizures with brainstem SD, however, severe local hypoxia ($pO_2 < 10$ mmHg) occurred that extended into the postictal period for both non-fatal and fatal seizures (pO_2 nadir: 1.8 \pm 0.9 mmHg and 0 \pm 0 mmHg, respectively; Fig. 7E,F). Hypoxia lasted 34 – 74 s for non-fatal cases ($n = 3$) and was followed by a period of hyperoxia (Fig. 7G). No pO_2 recovery occurred in fatal cases (Fig. 7H). SD in PCRT-r always preceded severe local hypoxia by 29 \pm 3.1 s, whereas VLM SD preceded hypoxia in the majority of seizures (5/7; Fig. 7I), by 5.4 \pm 3.2 s.

FIGURE 7. Seizure-induced brainstem spreading depolarization (SD) precedes local severe hypoxia in *Cacna1a*^{S218L} mice.

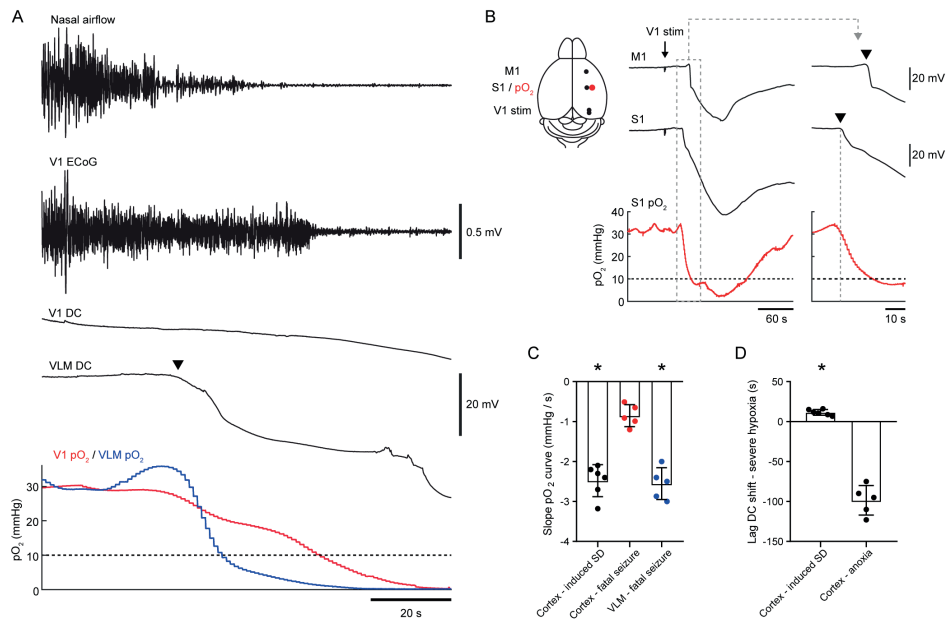


(A) Top and sagittal view of experimental approach for parallel brainstem pO_2 (red) and DC-recordings (PCRt = parvocellular reticular nucleus; VLM = ventrolateral medulla). (B) Nissl staining showing the track of an oxygen-sensing probe close to the VLM. (C) Example interictal VLM pO_2 recordings for 3 *Cacna1a*^{S218L} mice, which remained within the normoxic range of 20 – 40 mmHg. (D–F) Example recordings during termination of IC-induced seizures, including a non-fatal seizure not showing sudden changes in brainstem DC-potential (D) and a non-fatal (E) and fatal seizure (F) during which brainstem SD (arrowheads) occurred. Recordings of local VLM pO_2 (bottom) indicate severe hypoxia ($pO_2 < 10$ mmHg; shaded red) during brainstem SD. (G) Expanded timescale of pO_2 measurements during the non-fatal seizure presented in (E), showing rebound hyperoxia for minutes following initial severe hypoxia (red dotted line). (H) Average pO_2 during VLM SD (onset at time = 0; $n = 3$ non-fatal and $n = 4$ fatal seizures). Recovery from severe hypoxia (red dotted line) occurred only for non-fatal seizures. (I) Time lag between onset of SD in PCRt-r and VLM and severe hypoxia. All PCRt-r SDs and the majority of VLM SDs preceded hypoxia.

To confirm that the early hypoxia observed in the brainstem was a local effect, we measured pO_2 simultaneously in both V1 cortex and VLM in a subset of animals. Baseline cortical pO_2 was similar to baseline pO_2 levels observed in VLM (32.3 ± 2.5 mmHg). During fatal seizures ($n = 5$) severe hypoxia in VLM occurred in close association with VLM SD and preceded severe cortical hypoxia

by 25 – 38 s (example in Fig. 8A). In a separate group of *Cacna1a*^{S218L} mice ($n = 4$), cortical pO₂ dynamics during electrically induced cortical SD (Fig. 8B) confirmed that the pO₂ monitoring system was capable of detecting shifts in pO₂ coinciding with SD, with severe hypoxia detected after 7 – 16 s. Furthermore, pO₂ decreases were more abrupt during induced cortical SDs and SDs in the VLM associated with evoked fatal seizures, when compared to cortical recordings during fatal seizures not associated with cortical SD (Fig. 8C). Finally, cortical DC shifts did occur >60 s after a fatal seizure and long after severe hypoxia had commenced, indicative of anoxic depolarization (AD; Fig. 8D). These data indicate that the pO₂ dynamics measured in the brainstem reflect pO₂ changes induced by local SD, which are distinct from pO₂ dynamics preceding AD.

FIGURE 8. Oxygen dynamics in the ventrolateral medulla indicate that hypoxia is induced by brainstem spreading depolarization (SD) in *Cacna1a*^{S218L} mice.



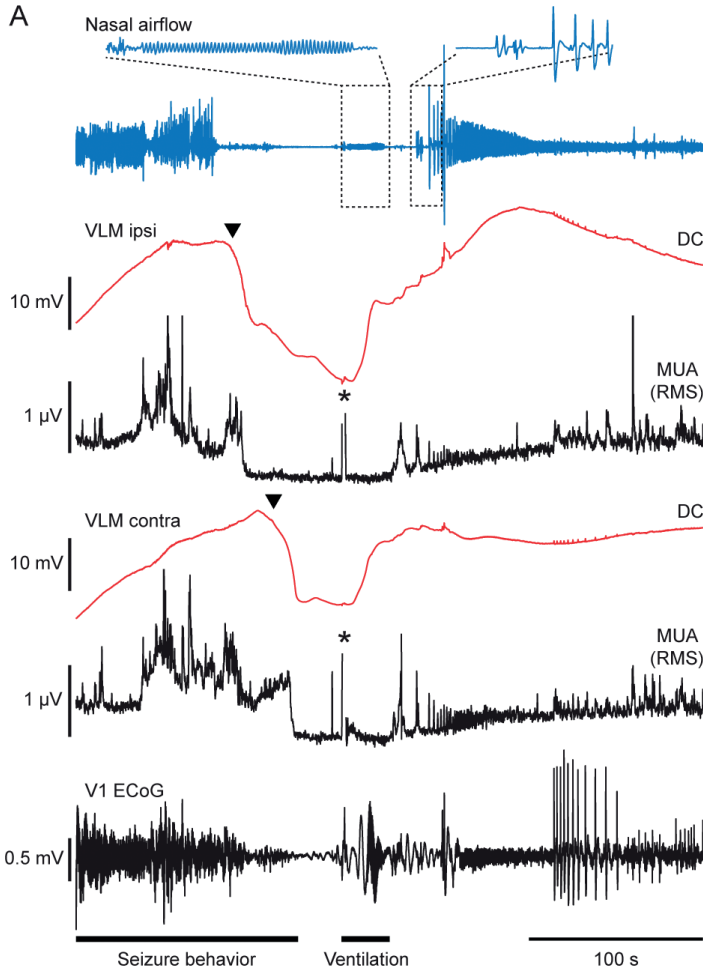
(A) Example of a fatal seizure with parallel pO₂ measurements in the ventrolateral medulla (VLM, blue) and primary visual cortex (V1, red). In this example, severe hypoxia (dashed line) in the VLM preceded cortical hypoxia by 25 s. **(B)** Schematic (left) showing experimental approach for cortical stimulation in freely behaving mice (M1 = primary motor cortex; S1 = primary somatosensory cortex). Cathodal stimulation in the primary visual cortex (V1 stim) resulted in a sequential DC shift in S1 and M1. SD in S1 coincided with a drop in pO₂ (right; arrowheads indicate SD onset), followed by severe hypoxia (10 mmHg, dashed horizontal line) 15 s after SD onset in this example. **(C)** Maximum pO₂ slope measured in 5-s bins indicating a more abrupt decrease in pO₂ for DC shifts during cortically induced SD (black; 6 SDs in $n = 4$ mice, 1 – 2 SDs per mouse) and VLM SD (blue), when compared to cortical pO₂ during fatal seizures (red; $t(9) = 7.69$ and $t(8) = 7.88$ respectively, $*p < 0.0001$, unpaired t -tests). **(D)** For cortical recordings, severe hypoxia occurred closer to DC shifts associated with cortically induced SD when compared to DC shifts associated with anoxia following fatal seizures ($t(9) = 14.4$, $*p < 0.0001$, unpaired t -test).

Fatality following brainstem SD can be prevented by timely respiratory resuscitation

In previous experiments, MUA recovery following VLM SD was observed after 26 ± 8 s (range 15 – 54) and 44 ± 5 s (range: 29 – 62) for spontaneous and induced non-fatal seizures, respectively. We therefore considered VLM SD without MUA recovery within 60 s fatal, and initiated mechanical ventilation >60 s after SD onset. This led to successful resuscitation in 7/9 animals (65 – 79 s for successful attempts; 70 and 76 s for non-successful attempts). During resuscitation, DC-potential recovery in the VLM was observed, that always preceded the first gasp (Fig. 9A). Bradypnea duration in the 7 resuscitated animals was 132 ± 10 s (range: 104 – 180), significantly longer than in animals with spontaneous recovery ($n = 12$; 75 ± 5 s [range: 75 – 102]; $t(17) = 6.21$, $p < 0.0001$, unpaired t -test). Breathing did not recover in animals receiving sham ventilation ($n = 3$; 61, 72 and 80 s after SD onset) or mechanical ventilation initiated >80 s after bradypnea onset ($n = 3$; 81, 91 and 102 s after SD onset).

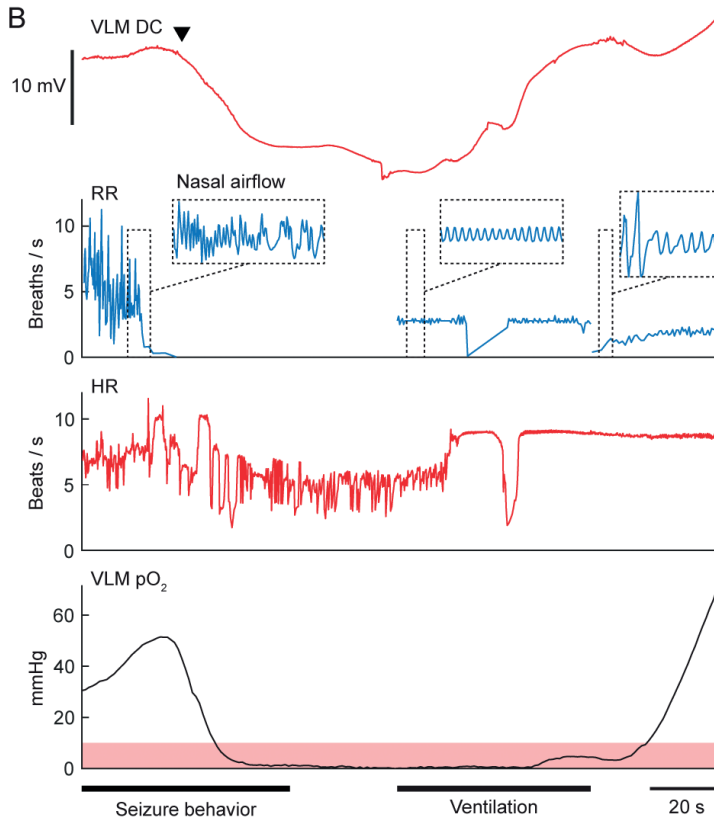
Finally, 3 mice implanted with a brainstem oxygen-sensing probe were mechanically ventilated at 62 – 65 s following VLM SD onset. In all animals, an increase in heart rate, recovery of VLM DC-potential and spontaneous breathing activity preceded recovery from severe hypoxia (example in Fig. 9B). In compliance with respiratory data, hypoxic burden, measured by the area below 10 mmHg³¹ was greater in resuscitated animals than in animals with spontaneous recovery (752 – 1580 mmHg*s and 151 – 523 mmHg*s, respectively; both $n = 3$).

FIGURE 9A. Respiratory resuscitation following spreading depolarization (SD) in ventrolateral medulla (VLM) prevents fatal outcome in *Cacna1a*^{S218L} mice.



(A) Example of a successful resuscitation attempt after bilateral VLM SD (arrowheads) following inferior colliculus (IC) stimulation. Mechanical ventilation was commenced 70 s after VLM SD onset in this case, in absence of spontaneous DC and multi-unit activity (MUA) recovery. Effective delivery of air was confirmed by a regular oscillatory nasal airflow signal (inset top left), and was always accompanied by early recovery of VLM DC-potential, followed by MUA recovery. Respiratory activity invariably resumed with gasping (inset top right). Asterisks denote artifacts due to positioning of the animal for mechanical ventilation (RMS = root mean square; V1 ECoG = electrocorticogram in primary visual cortex).

FIGURE 9B. Respiratory resuscitation following spreading depolarization (SD) in ventrolateral medulla (VLM) prevents fatal outcome in *Cacna1a*^{S218L} mice.



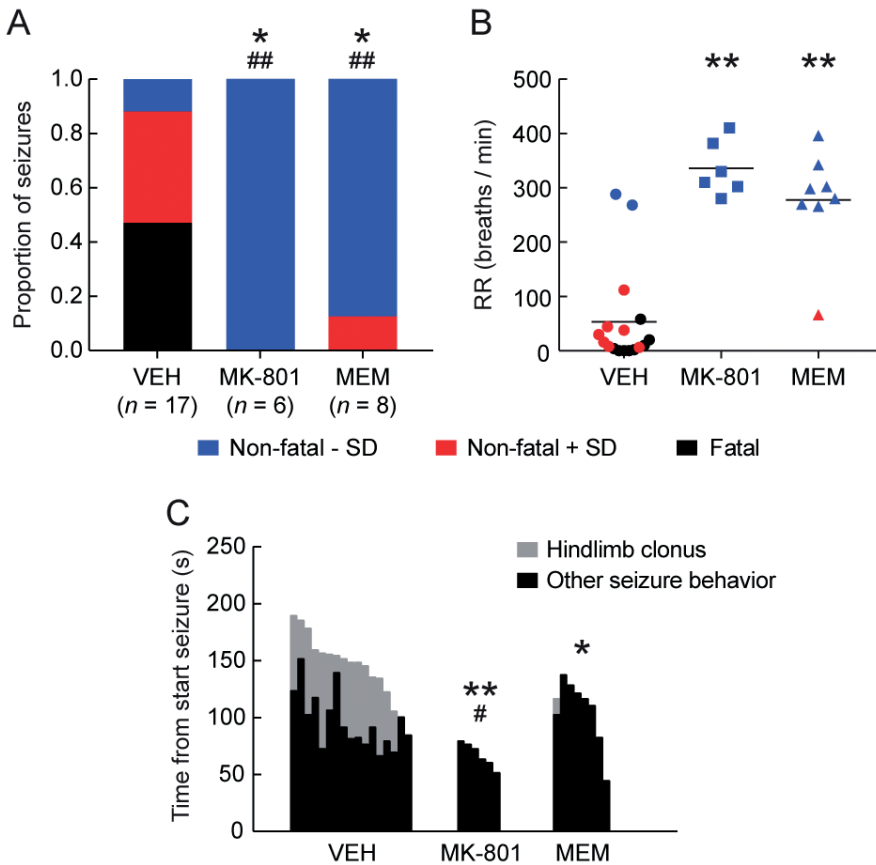
(B) Example of heart rate (HR) and local pO_2 changes during mechanical ventilation after VLM SD (arrowhead), showing that recovery of HR and VLM DC precedes recovery of local pO_2 . Note that effective ventilation was unintentionally interrupted in this case, as indicated by the transient drop in respiratory rate (RR). Severe hypoxia ($pO_2 < 10 \text{ mmHg}$) is indicated in shaded red.

NMDA receptor antagonists prevent seizure-induced brainstem SD and fatality

In vitro and *in vivo* studies showed that blockade of NMDA receptors by MK-801 inhibits locally induced brainstem SD.^{11, 32} We tested whether seizure-induced brainstem SD and respiratory compromise can be prevented by treatment with MK-801 (1 mg/kg) preceding IC stimulation. Irrespective of treatment, all animals showed a stage 5 seizure. However, MK-801 prevented brainstem SD, bradypnea and fatal outcome (Fig. 10A,B). Upon recovery of seizures, however, mice demonstrated loss of postural control and hyperactive limb movements for up to 2 h following MK-801 injection. We therefore also tested the effects of memantine, a clinically well-tolerated

NMDA receptor antagonist.^{33, 34} Memantine (10 mg/kg) prevented mortality and, in all but 1 mouse, brainstem SD and bradypnea (Fig. 10A,B) and did not result in overt peri-ictal behavioral changes. Absence of hindlimb clonus, that specifically occurred during termination of spontaneous and induced seizures displaying VLM SD, accounted for a shorter seizure duration for memantine-treated, but not MK-801-treated, mice (Fig. 10C).

FIGURE 10. NMDA receptor antagonists prevent seizure-induced medullary spreading depolarization (SD), respiratory suppression and fatal outcome in *Cacna1a*^{S218L} mice.



Cacna1a^{S218L} mice received acute intraperitoneal treatment with vehicle (VEH), MK-801 (1 mg/kg), or memantine (MEM, 10 mg/kg) 30 min prior to an inferior colliculus stimulation-induced seizure. **(A)** Proportion of seizures with fatal or non-fatal outcome, with or without SD in the ventrolateral medulla (VLM). Note that all fatal seizures were associated with VLM SD. Animals pretreated with MK-801 or MEM had seizures that were significantly less likely fatal ($*p < 0.05$, χ^2 test) and less likely associated with VLM SD ($^{##}p < 0.001$, χ^2 test). **(B)** Mean respiratory rate (RR) during the last minute of seizure behavior, indicating respiratory suppression during seizures with VLM SD (red and black). RR was significantly greater for animals pretreated with MK-801 or MEM ($^{***}p < 0.0001$, ANOVA with Dunnett's test). **(C)** Seizures were significantly shorter for animals pretreated with MK-801 or MEM ($^{**}p = 0.001$ and $*p = 0.013$, respectively, ANOVA with Dunnett's test). When excluding hindlimb clonus (grey), MK-801 pretreatment resulted in shorter seizures while MEM did not ($*p = 0.045$ and $p = 0.755$, respectively, ANOVA with Dunnett's test). Hindlimb clonus only occurred for seizures associated with VLM SD (VEH: $n = 15$; MEM: $n = 1$).

DISCUSSION

Here we show that spreading depolarization (SD) causes respiratory compromise and apnea upon invasion of the brainstem ventrolateral medulla (VLM) during spontaneous and induced seizures in *Cacna1a*^{S218L} mice. Incidence, onset and recovery of SD in the VLM was strongly related to apnea and SD was not caused by local hypoxia but instead *initiated* such hypoxia. We confirmed that putative fatal SD and subsequent hypoxia were reversible by resuscitation. Furthermore, prevention of SD initiation by NMDA receptor antagonists confirmed that SD is a prerequisite for seizure-related apnea in this animal model.

Cacna1a^{S218L} mice have been proposed as a SUDEP model as homozygotes present spontaneous non-fatal and fatal tonic-clonic seizures at different ages.¹³ Here we show that prolonged seizure-related apnea frequently occurs in this genetic mouse model. Data from rare monitored SUDEP cases indicate that apnea precedes cardiac arrest.⁴ In patients with implanted electrodes aberrant activity in the amygdala, either caused by a seizure or electrical stimulation, was associated with apnea.³⁵ Although this revealed a potential mechanism of seizure-related apnea, breathing resumed before seizure termination, suggesting that other or additional mechanisms are involved in SUDEP as apnea in the postictal period appears dangerous.^{3,4}

In the present study, recording electrodes were located in or near the ventral respiratory column, at the level of the pre-Bötzinger Complex (preBötC). PreBötC neurons are essential for breathing rhythm¹⁵ and the respiratory response to hypoxia.^{16,17} Rapid suppression of glutamatergic preBötC neurons induces lethal apnea,¹⁹ whereas unilateral stimulation of inhibitory preBötC populations is sufficient to induce apnea during the stimulation period.³⁶ Our data indicate that neuronal suppression in the VLM following SD induces apnea, and subsequently hypoxia: i) VLM SD occurred specifically during seizures with bradypnea, ii) bradypnea did not occur during seizures with SD limited to the rostral brainstem (PnO), iii) the timing of bradypnea correlated well with neuronal suppression in the VLM, but not with neuronal suppression in the PnO, and iv) brainstem hypoxia occurred in association with brainstem SD and preceded cortical hypoxia. Variations in onset of VLM SD relative to bradypnea may be explained by small deviations in electrode position (~200 µm), as SD propagation is known to be especially slow in brainstem areas.³²

Our findings corroborate previous studies that reported brainstem SD in different SUDEP animal models.¹¹⁻¹³ Based on DC-potential recordings in the dorsal medulla, it was proposed that brainstem SD occurred in the postictal period, secondary to ictal hypoxia as fatal apnea was already present upon detection of brainstem SD.^{11,12} Whereas this provides a rationale for the absence of successful autoresuscitation efforts during fatal seizures in SUDEP mouse models,^{13,37} it does not explain the onset of apnea. In the present study, brainstem SD preceded apnea, which may be explained by the different location of the brainstem recording electrode. Previously, this electrode was positioned in the dorsocaudal medulla that is primarily involved in cardiovascular function,^{11,12} while we placed the electrode in the ventrolateral medulla that is primarily involved in respiratory

function. As such, VLM SD may be the underlying mechanism for both the onset of apnea and the absence of autoresuscitation efforts.

Our data indicate that hypoxia is a consequence, rather than a cause, of seizure-related brainstem SD: i) SD was detected rostral and immediately caudal from the brainstem oxygen probe at respectively ~30 s and ~5 s preceding local hypoxia, whereas we found that AD occurred after >60 s following severe hypoxia, in line with a previous study showing AD in the hyperexcitable brainstem after ~60 s,³⁰ ii) pO₂ decreases were more abrupt in brainstem than in cortex in the absence of cortical SD, but similar to pO₂ decreases after cortical SD, which may be explained by increased local metabolic demand during SD³⁸ and iii) NMDA antagonists prevented seizure-induced brainstem SD, as shown for locally induced SD,^{11, 32} but do not delay cortical AD.³⁹ Together, this indicates that brainstem hyperexcitability rather than hypoxia initiates seizure-related brainstem SD.

Differences in seizure networks between SUDEP animal models may be crucial in determining the events leading to death. The seizure phenotype in *Cacna1a*^{S218L} mice suggests an important role for brainstem networks,¹³ confirmed here by the similar seizure phenotype following IC stimulation. Surgery reduced survival which may be due to an increased risk of SD following tissue trauma, although implanted animals show similar seizures as naïve animals.¹³ Seizures associated with cortical epileptiform activity were prolonged (lasting >30 min), whereas we observed forebrain SDs only during half of the fatal seizures, supporting the premise that increased brainstem network excitability is necessary and sufficient for the (lethal) seizures observed in *Cacna1a*^{S218L} mice. Although brainstem networks have not been extensively studied for seizures in other models, decreased thresholds for SD implying hyperexcitable brainstem networks were found in multiple SUDEP animal models.^{11, 12} Endogenous brainstem activity was sufficient for hyperthermia- and kainate-induced convulsive seizures in infant rats after precollicular transection.⁴⁰ Furthermore, in a mouse model of acquired temporal lobe epilepsy, increased excitability was found in the nucleus tractus solitarius.⁴¹ These preclinical studies implicate brainstem hyperexcitability in SUDEP pathophysiology. However, to generalize our findings, studies in other models are needed that investigate VLM SD in relation to respiratory suppression and hypoxia.

Longer VLM SD duration for fatal seizures was associated with prolonged suppression of local neuronal activity and breathing. Resuscitation resulted in sequential recovery of heart rate, VLM DC-potential, VLM neuronal activity and breathing activity. Interestingly, VLM DC-potential always recovered before VLM pO₂, suggesting that perfusion pressure rather than tissue oxygenation is crucial for initial recovery of brainstem SD, as reported previously for cortical SD.⁴² Resuscitation was initiated in a time-window that indicated fatal outcome. Earlier studies initiated resuscitation after a few seconds of apnea^{37, 43} or directly after seizure induction.⁴⁴ Our data extend these findings and suggest that ventilatory support is sufficient to recover brainstem control of respiratory function during prolonged apnea.

Only non-fatal seizures with VLM SD were associated with apnea. We are unaware of descriptions of prolonged apnea during and following non-fatal seizures in other animal models,

although in clinical epilepsy hypoxemia is common.² Other than respiratory effects, non-fatal seizures with brainstem SD could be discriminated from other non-fatal seizures by postictal ECoG suppression and increased HRV. As non-fatal seizures with brainstem SD were associated with a shorter time towards a fatal seizure, these postictal dynamics may be of clinical interest. Increases in pre- and interictal HRV were found in a patient one day prior to a cluster of seizures leading to SUDEP.⁴⁵ These and other potential biomarkers, including post-convulsive central apnea³ and imaging data implicating atrophy in the mesencephalon and medulla oblongata,^{8,9} may improve SUDEP risk assessment.

Our data showed that hindlimb clonus was specific for seizures with VLM SD and displayed strong overlap in timing with SD. This suggests that hindlimb clonus can be the result of SD-induced motor system activation, for example via reticulospinal pathways.⁴⁶ In SUDEP cases, apnea and asystole appear to occur postictally.⁴ The obvious difference in brainstem dimensions in humans *versus* mice and the slow propagation of SD complicates translation of the observed motor effects to patients. SD-induced behavior and cardiorespiratory collapse may thus have different temporal sequences across species.

Treatment with NMDA receptor antagonists MK-801 or memantine did not affect seizure stage, yet total seizure duration was significantly decreased. Although this decrease was largely attributed to the absence of SD-induced hindlimb clonus, duration *per se* may be a poor predictor of seizure outcome. Indeed, we found no differences in duration of spontaneous seizures with and without brainstem SD in *Cacna1a*^{S218L} mice. Clinical data in fact indicate the contrary, as postictal central apnea is more common for shorter seizures.³ Activation of NMDA receptors by glutamate following postsynaptic depolarization is importantly implicated in SD.⁴⁷ Treatment with MK-801 or memantine largely abolished VLM SD and the associated apnea, thereby preventing fatal outcome. These findings suggest the potential of an NMDA receptor antagonist as preventative treatment option in individuals with a high SUDEP risk. Importantly, clinical evidence for seizure-related brainstem SD is crucial before considering such an approach.

REFERENCES

1. Nashef, L., et al., Apnoea and bradycardia during epileptic seizures: relation to sudden death in epilepsy. *J Neurol Neurosurg Psychiatry*, 1996. 60(3): p. 297-300.
2. Bruno, E., et al., Ictal hypoxemia: A systematic review and meta-analysis. *Seizure*, 2018. 63: p. 7-13.
3. Vilella, L., et al., Postconvulsive central apnea as a biomarker for sudden unexpected death in epilepsy (SUDEP). *Neurology*, 2019. 92(3): p. e171-e182.
4. Ryvlin, P., et al., Incidence and mechanisms of cardiorespiratory arrests in epilepsy monitoring units (MORTEMUS): a retrospective study. *Lancet Neurol*, 2013. 12(10): p. 966-77.
5. Massey, C.A., et al., Mechanisms of sudden unexpected death in epilepsy: the pathway to prevention. *Nat Rev Neurol*, 2014. 10(5): p. 271-82.
6. Devinsky, O., et al., Sudden unexpected death in epilepsy: epidemiology, mechanisms, and prevention. *Lancet Neurol*, 2016. 15(10): p. 1075-88.
7. Harden, C., et al., Practice guideline summary: Sudden unexpected death in epilepsy incidence rates and risk factors: Report of the Guideline Development, Dissemination, and Implementation Subcommittee of the American Academy of Neurology and the American Epilepsy Society. *Neurology*, 2017. 88(17): p. 1674-1680.
8. Mueller, S.G., L.M. Bateman, and K.D. Laxer, Evidence for brainstem network disruption in temporal lobe epilepsy and sudden unexplained death in epilepsy. *Neuroimage Clin*, 2014. 5: p. 208-16.
9. Mueller, S.G., et al., Brainstem network disruption: A pathway to sudden unexplained death in epilepsy? *Hum Brain Mapp*, 2018. 39(12): p. 4820-4830.
10. Patodia, S., et al., The ventrolateral medulla and medullary raphe in sudden unexpected death in epilepsy. *Brain*, 2018. 141(6): p. 1719-1733.
11. Aiba, I. and J.L. Noebels, Spreading depolarization in the brainstem mediates sudden cardiorespiratory arrest in mouse SUDEP models. *Sci Transl Med*, 2015. 7(282): p. 282ra46.
12. Aiba, I., X.H. Wehrens, and J.L. Noebels, Leaky RyR2 channels unleash a brainstem spreading depolarization mechanism of sudden cardiac death. *Proc Natl Acad Sci U S A*, 2016. 113(33): p. E4895-903.
13. Loonen, I.C.M., et al., Brainstem spreading depolarization and cortical dynamics during fatal seizures in *Cacna1a* S218L mice. *Brain*, 2019. 142(2): p. 412-425.
14. Smith, J.C., et al., Brainstem respiratory networks: building blocks and microcircuits. *Trends Neurosci*, 2013. 36(3): p. 152-62.
15. Del Negro, C.A., G.D. Funk, and J.L. Feldman, Breathing matters. *Nat Rev Neurosci*, 2018. 19(6): p. 351-367.
16. Gray, P.A., et al., Normal breathing requires preBotzinger complex neurokinin-1 receptor-expressing neurons. *Nat Neurosci*, 2001. 4(9): p. 927-30.
17. McKay, L.C., W.A. Janczewski, and J.L. Feldman, Sleep-disordered breathing after targeted ablation of preBotzinger complex neurons. *Nat Neurosci*, 2005. 8(9): p. 1142-4.
18. Feldman, J.L. and C.A. Del Negro, Looking for inspiration: new perspectives on respiratory rhythm. *Nat Rev Neurosci*, 2006. 7(3): p. 232-42.

19. Tan, W., et al., Silencing preBotzinger complex somatostatin-expressing neurons induces persistent apnea in awake rat. *Nat Neurosci*, 2008. 11(5): p. 538-40.
20. van den Maagdenberg, A.M., et al., High cortical spreading depression susceptibility and migraine-associated symptoms in Ca(v)2.1 S218L mice. *Ann Neurol*, 2010. 67(1): p. 85-98.
21. McAfee, S.S., et al., Minimally invasive highly precise monitoring of respiratory rhythm in the mouse using an epithelial temperature probe. *J Neurosci Methods*, 2016. 263: p. 89-94.
22. Griffiths, J.R. and S.P. Robinson, The OxyLite: a fibre-optic oxygen sensor. *Br J Radiol*, 1999. 72(859): p. 627-30.
23. Houben, T., et al., Optogenetic induction of cortical spreading depression in anesthetized and freely behaving mice. *J Cereb Blood Flow Metab*, 2017. 37(5): p. 1641-1655.
24. Racine, R.J., Modification of seizure activity by electrical stimulation. II. Motor seizure. *Electroencephalogr Clin Neurophysiol*, 1972. 32(3): p. 281-94.
25. Trinka, E., et al., A definition and classification of status epilepticus--Report of the ILAE Task Force on Classification of Status Epilepticus. *Epilepsia*, 2015. 56(10): p. 1515-23.
26. Nashef, L., et al., Unifying the definitions of sudden unexpected death in epilepsy. *Epilepsia*, 2012. 53(2): p. 227-33.
27. Thireau, J., et al., Heart rate variability in mice: a theoretical and practical guide. *Exp Physiol*, 2008. 93(1): p. 83-94.
28. McCown, T.J., et al., Electrically elicited seizures from the inferior colliculus: a potential site for the genesis of epilepsy? *Exp Neurol*, 1984. 86(3): p. 527-42.
29. Faingold, C.L., Brainstem Networks: Reticulo-Cortical Synchronization in Generalized Convulsive Seizures, in Jasper's Basic Mechanisms of the Epilepsies, J.L. Noebels, et al., *Editors*. 2012: Bethesda (MD).
30. Richter, F., et al., The relationship between sudden severe hypoxia and ischemia-associated spreading depolarization in adult rat brainstem in vivo. *Exp Neurol*, 2010. 224(1): p. 146-54.
31. Farrell, J.S., et al., Postictal behavioural impairments are due to a severe prolonged hypoperfusion/hypoxia event that is COX-2 dependent. *Elife*, 2016. 5.
32. Richter, F., et al., Spreading depression in the brainstem of the adult rat: electrophysiological parameters and influences on regional brainstem blood flow. *J Cereb Blood Flow Metab*, 2008. 28(5): p. 984-94.
33. Bullock, R., Efficacy and safety of memantine in moderate-to-severe Alzheimer disease: the evidence to date. *Alzheimer Dis Assoc Disord*, 2006. 20(1): p. 23-9.
34. Winblad, B., et al., Memantine in moderate to severe Alzheimer's disease: a meta-analysis of randomised clinical trials. *Dement Geriatr Cogn Disord*, 2007. 24(1): p. 20-7.
35. Dlouhy, B.J., et al., Breathing Inhibited When Seizures Spread to the Amygdala and upon Amygdala Stimulation. *J Neurosci*, 2015. 35(28): p. 10281-9.
36. Sherman, D., et al., Optogenetic perturbation of preBotzinger complex inhibitory neurons modulates respiratory pattern. *Nat Neurosci*, 2015. 18(3): p. 408-14.
37. Kim, Y., et al., Severe peri-ictal respiratory dysfunction is common in Dravet syndrome. *J Clin Invest*, 2018. 128(3): p. 1141-1153.

38. Takano, T., et al., Cortical spreading depression causes and coincides with tissue hypoxia. *Nat Neurosci*, 2007. 10(6): p. 754-62.
39. Lauritzen, M. and A.J. Hansen, The effect of glutamate receptor blockade on anoxic depolarization and cortical spreading depression. *J Cereb Blood Flow Metab*, 1992. 12(2): p. 223-9.
40. Pospelov, A.S., et al., Forebrain-independent generation of hyperthermic convulsions in infant rats. *Epilepsia*, 2016. 57(1): p. e1-6.
41. Derera, I.D., B.P. Delisle, and B.N. Smith, Functional Neuroplasticity in the Nucleus Tractus Solitarius and Increased Risk of Sudden Death in Mice with Acquired Temporal Lobe Epilepsy. *eNeuro*, 2017. 4(5).
42. Sukhotinsky, I., et al., Perfusion pressure-dependent recovery of cortical spreading depression is independent of tissue oxygenation over a wide physiologic range. *J Cereb Blood Flow Metab*, 2010. 30(6): p. 1168-77.
43. Faingold, C.L., M. Randall, and S. Tupal, DBA/1 mice exhibit chronic susceptibility to audiogenic seizures followed by sudden death associated with respiratory arrest. *Epilepsy Behav*, 2010. 17(4): p. 436-40.
44. Buchanan, G.F., et al., Serotonin neurones have anti-convulsant effects and reduce seizure-induced mortality. *J Physiol*, 2014. 592(19): p. 4395-410.
45. Jeppesen, J., et al., Heart rate variability analysis indicates preictal parasympathetic overdrive preceding seizure-induced cardiac dysrhythmias leading to sudden unexpected death in a patient with epilepsy. *Epilepsia*, 2014. 55(7): p. e67-71.
46. Hirsch, E., et al., Generalized seizures: from clinical phenomenology to underlying systems and networks. 2006: John Libbey Eurotext.
47. Dreier, J.P., The role of spreading depression, spreading depolarization and spreading ischemia in neurological disease. *Nat Med*, 2011. 17(4): p. 439-47.